Dual-Band Power Divider with Wide Suppression Band: Artificial Intelligence Modeling for Performance Confirmation

Golshan Mohamadpour[1], Salman Karimi[1†] and Saeed Roshani[2]

[1]Department of Electrical Engineering, Lorestan University, Khorramabad, Iran

[2]Department of Electrical Engineering, Kermanshah Branch, Islamic Azad University, Kermanshah, Iran

***Abstract*—In this paper, a planar dual-band Wilkinson power divider (DWPD) with a triangular-shaped resonator is designed. This work stands out from existing designs by addressing key limitations in conventional power dividers, i.e., physical size, harmonic suppression, and insertion loss. The proposed triangular-shaped resonator has a compact size of 9.9 mm × 3.4 mm (0.26 λ_g × 0.09 λ_g), where λ_g is electrical wavelength at 5.9 GHz, and provides a wide suppression band from 7.1 GHz to 20.6 GHz with a 20 dB attenuation level. In the proposed DWPD structure, two triangular-shaped resonators are used in two branches. It works at 3.6 GHz and 5.5 GHz with <0.1 dB insertion loss at both operating bands. The input and output return losses and ports isolation parameters at both bands are better than 20 dB, which show good performance of the divider at operating bands. Besides the acceptable performance, the proposed DWPD provides a wide suppression band from 6.8 GHz to 20.5 GHz with more than 20dB attenuation level. In the divider design, the neural network is employed to model a triangular-shaped resonator. The proposed neural network has two outputs (S_{11} and S_{21}), and two hidden layers with eight neurons at each layer. The weights of each neuron are obtained using particle swarm optimization algorithms. The proposed neural network model has accurate results, and the mean relative error of the train and test data for both outputs is <0.1, which validates the accurate results of the proposed model.**

***Index Terms*—Dual band Wilkinson power divider, Harmonic suppression, Neural network, Resonator.**

I. Introduction

Power dividers are widely used component in microwave circuits and systems (Cheng and Law, 2008). This device divides input signals into two or more signals, and it is also a reciprocal device, so it can be used to combine power from output ports into the input port. A typical Wilkinson divider consists of two-quarter wavelength (λ/4) microstrip lines and a lumped 100 ohms' resistor between two lines in order to create port isolation. However, despite its wide applications, it has basic problems, which passes unwanted signals at other frequencies along with desired signal. In recent years, various designs are provided to remove undesirable harmonic.

Moreover, the typical divider operates only in a single band. Recently, various dual-band dividers are presented.

However, harmonic-suppressed dual-band dividers need high-tech and complex design. In (Srisathit, Chongcheawchamnan and Worapishet, 2003), (Wu, et al., 2005), and (Wu, et al., 2006), various dual-band power dividers based on open or short stubs and lumped elements are presented.

In (Srisathit, Chongcheawchamnan and Worapishet, 2003), a two-section transformer is used to create a dual-band divider, which has a simple structure but suffers from poor output ports isolation (S32) and poor output return losses (S22, S33). In (Wu, et al., 2005) and (Wu, et al., 2006), two dual bands divider are reported with lumped elements (L-C). The frequency response is improved in these dividers but they need extra fabrication process and frequency limitation due to applied lumped components.

As mentioned, the typical divider cannot suppress harmonics, but in the modern wireless communication systems, harmonics suppression is a necessary demand (Roshani, Roshani and Zarinitabar, 2019b), (Heydari and Roshani, 2017), (Liang and Xu, 2012), (Roshani, et al., 2018), therefore, several methods are introduced to overcome this drawback.

In many works, low pass filters (Mohammadi, et al., 2024), (Lotfi, Roshani and Roshani, 2020), and (Roshani, et al., 2016) and resonators (Heydari, Rostami and Roshani, 2019) and (Jamshidi, et al., 2019), are used to rejects unwanted harmonics. In these works, unwanted harmonics are successfully removed, but this method increases the insertion loss of the divider. Microstrip filters (Roshani, Dehghani, and Roshani, 2019a) are widely used in electronic systems

ARO-The Scientific Journal of Koya University
Vol. XIII, No. 1 (2025), Article ID: ARO.11945. 7 pages
DOI: 10.14500/aro.11945
Received: 13 December 2024; Accepted: 15 January 2025
Regular research paper; Published: 01 February 2025
†Corresponding author's email: karimi.salman@lu.ac.ir
Copyright © 2025 Golshan Mohamadpour, Salman Karimi and Saeed Roshani. This is an open-access article distributed under the Creative Commons Attribution License (CC BY-NC-SA 4.0).

to enhance the performance of both passive (Bavandpour, et al., 2021) and active devices by selectively passing desired frequency bands and suppressing unwanted signals. Their compact size, high efficiency, and ability to suppress harmonics make them integral to improving signal integrity and stability in applications such as wireless communications (Roshani, et al., 2023), radar, and satellite systems. In some other works, electromagnetic (EM) band gap cells (Lin, et al., 2007) and DGS (Woo and Lee, 2005) are used for harmonics suppression. Unfortunately, these methods need an extra fabrication process, which is undesirable. Lumped reactive components (external L and C), (MahdiAbadi, et al., 2024), (Pirasteh, Roshani and Roshani, 2020), (Huang, et al., 2010), (Wang, et al., 2014b), and (Wang, et al., 2014a) are used as other methods to overcome the presence of harmonics in the frequency response, which this approach is also undesirable for mass production environments.

Microstrip stubs, including open-ended or short-ended configurations, are widely used to suppress unwanted harmonics, as demonstrated in studies (Tang and Chen, 2016), (Wang, et al., 2017), (Cheng and Ip, 2010), and (Ahmed and Abbosh, 2015). These methods have a simple structure but suppress only a few harmonics.

Previously, several dividers with only harmonics suppression ability or dual band divider are designed and reported. However, previously only few dividers are designed, which have both properties of dual-band and harmonics suppression together.

In (Rostami and Roshani, 2018) a dual-band divider was designed at 0.9/1.8 GHz, which suppressed undesired signals from 3.1GHz to 10.6 GHz. In this work several lumped capacitors are used, restricting the operating frequency and also undesirable for mass production environments. In (Roshani, et al., 2022) a dual-band divider designed at 2.6/3.3 GHz, which only suppresses 3rd harmonics. This work exhibits a large insertion loss.

In recent years, artificial neural networks (ANN) are used to model and prediction of microwave device like divider as useful tools (Jamshidi, et al., 2020), (Yahya, et al., 2024), (Yahya, et al., 2022), and (Roshani, et al., 2021).

In this work, a harmonic suppressed Dual-band Wilkinson Power Divider (DWPD) is proposed using resonators, and the neural network models are used to model the desired parameters to improve the operation of resonators. The ADS simulator is used to simulate the resonator and divider, and also MATLAB R2017a is applied to model the proposed resonator with neural networks. The proposed Wilkinson power divider (WPD) stands out due to its unique design, incorporating triangular-shaped resonators and advanced neural network modeling. This innovative approach allows the divider to operate efficiently in two frequency bands while achieving outstanding harmonic suppression. It effectively filters out unwanted signals across a wide range, from 7.1 GHz to 20.6 GHz, with more than 20 dB attenuation, all while maintaining a compact and efficient design with minimal signal loss. The use of neural networks ensures precise modeling of the resonators, enhancing the overall accuracy and performance of the system, making it a highly effective solution for modern microwave applications.

II. Power Divider Design Process

This section describes the design process of the typical divider and the proposed divider.

A. Typical WPD

A typical divider, as shown in Fig. 1 is composed of three ports, one port as input and two ports as output. The input port is connected to output ports with two long quarter-wave lines. There is a lumped resonator between two output ports in order to provide port isolation. Input signal at port 1 is divided into two output ports. In the typical divider, undesired signals at higher frequencies are passed with desired signal without any suppression, which has undesirable effects on the original signal. In the modern power dividers, the divider should pass the original signal at operating frequency and eliminate higher frequencies.

The conventional Wilkinson divider inherently lacks the ability to suppress harmonics because its λ/4 transmission lines are designed to operate at a single frequency. These lines allow higher-order harmonics to pass through alongside the desired signal, leading to interference and signal distortion. This limitation becomes increasingly problematic in modern applications that demand high signal integrity across multiple bands.

Conventional Wilkinson dividers typically exhibit low insertion loss within their operating band due to their simple structure of λ/4 transmission lines, and this parameter is defined by S_{12}. However, their port isolation and return loss performance often degrade outside this narrow frequency range. Port isolation, defined by $S_{23,}$ is generally sufficient at the design frequency but is not optimized for dual-band or wideband operations. Similarly, return losses, measured at the input and output ports (S_{11}, S_{22}, and S_{33}), are acceptable in single-band applications but decline significantly for higher-order harmonics.

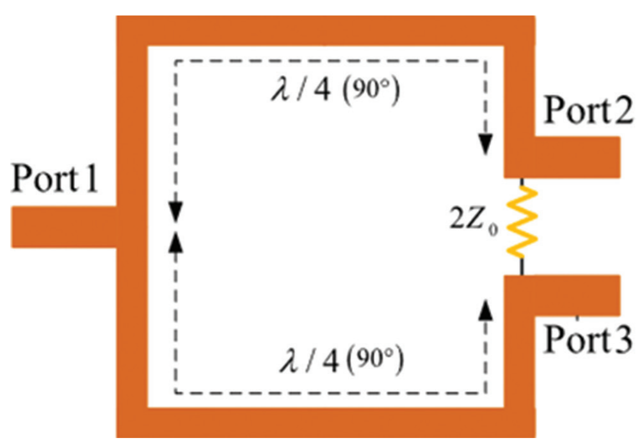

Fig. 1. Structure of a conventional Wilkinson power divider with λ/4 branches and a 100-ohm isolation resistor.

B. Proposed WPD Design

The block diagram of the proposed divider to suppress unwanted harmonics is depicted in Fig. 2. In this structure, two small resonators should be inserted in two branches of the typical divider. These resonators should pass the original signal at the operating frequency with low insertion loss and suppress other signals at higher frequencies.

In the proposed Wilkinson Divider design, which is illustrated in Fig. 2, the long conventional λ/4 branches are replaced with a novel structure that combines a resonator and two microstrip lines. These microstrip lines have an impedance of Z_1 and an electrical length of θ_1, resulting in a significantly smaller physical size compared to traditional λ/4 branches. This compact design not only reduces the overall footprint but also enhances harmonic suppression and operating efficiency. In addition, a lumped resistor, typically 100 ohms, is placed between Port 2 and Port 3 to ensure proper isolation between the output ports. This resistor plays a critical role in preventing signal interference and ensuring stable and reliable operation of the power divider across its intended frequency range.

C. Proposed Resonator Design

The structure of the proposed resonator, shown in (Fig. 3a), is designed to optimize performance by combining different impedance characteristics and stubs. It consists of three distinct sections: A central section and two outer sections. The central part of the resonator is designed with three high-low impedance sections, which create a balanced structure for impedance matching. This variation in impedance is essential for enhancing the performance of the resonator to operate efficiently over a range of frequencies, improving its overall performance in the system. In the two outer sections, long meandered lines are used. These meandering lines are loaded with rectangular shapes to further tune the resonance properties of the resonator. The meandered structure increases the effective length of the lines without occupying too much physical space, allowing for a compact design while still maintaining the desired electrical characteristics. The addition of rectangular shapes in these sections helps in controlling the resonant frequency and fine-tuning the response of the resonator. This combination of different impedance regions and the meandered line geometry ensures that the resonator can achieve the required resonance behavior while maintaining a compact and efficient design. Each section is chosen to contribute to the desired functionality and performance of the resonator in the proposed system. The proposed resonator is designed based on RT/Duroid substrate with $\varepsilon_r = 2.2$.

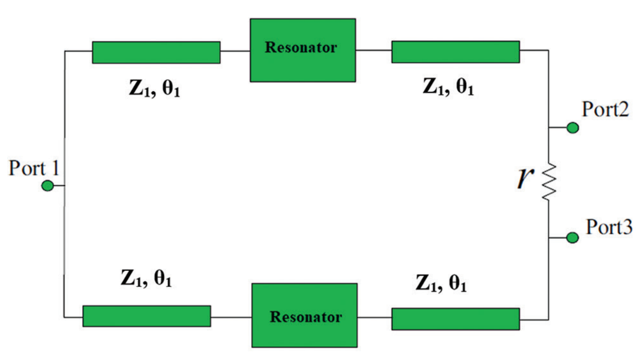

Fig. 2. Block diagram of the proposed dual-band Wilkinson power divider (WPD) with compact resonator-based branches.

The RT/Duroid substrate was chosen for its low dielectric constant and loss tangent, ensuring high performance at microwave frequencies. While it offers excellent signal integrity, its cost and scalability may pose challenges for large-scale production. Alternative materials could be considered for cost-sensitive applications in future work.

The compact size of the design inherently contributes to energy efficiency by reducing material usage and potentially lowering energy consumption during production. In addition, the enhanced performance and harmonic suppression can lead to more efficient operation in communication systems, indirectly reducing power waste.

The S-parameters of the designed resonator are depicted in (Fig. 3b) and phase curve of the proposed resonator is depicted in (Fig. 3c). As the results show, this resonator passes signals below 5.8 GHz with low insertion loss (IL) and provide wide rejection band from 7.1 GHz to 20.6 GHz with more than 20 dB suppression level.

III. Modeling of the Proposed resonator

The proposed resonator contains several high and low impedances, and making analysis and deriving closed-form equations for this structure is so difficult, therefore, an ANN model is provided for the proposed resonator.

The provided ANN model for the proposed resonator is depicted in Fig. 4. In the first step, inputs and outputs of the ANN model should be determined. For the designed resonator, the S_{11} and S_{12} are defined as the output of ANN model. In the resonators 4 parameters of W_1, L_1, W_2, and L_2 have important effect on the response, so these four parameters and frequency are considered as 5 inputs of the ANN model. The applied resonator is designed using EM simulation in ADS software and required data of ANN model are extracted from EM simulation in ADS. An multi-layer perceptron (MLP) with two hidden layers is used for provided ANN model.

Model details, including the number of input/output neurons and hidden layers, number of epochs, and activation functions are listed in Table I.

The ANN model used in the design of the proposed WPD plays a crucial role in accurately modeling and optimizing the triangular-shaped resonators. This approach ensures a precise relationship between the resonator's physical dimensions and its electrical performance, making the design both efficient and reliable.

The ANN model is based on a MLP structure with two hidden layers, each containing eight neurons. The input layer accepts five parameters—frequency and the key geometric parameters of the resonator (W_1, W_2, L_1, and L_2)—whereas the output layer predicts the S-parameters S_{11} (input return

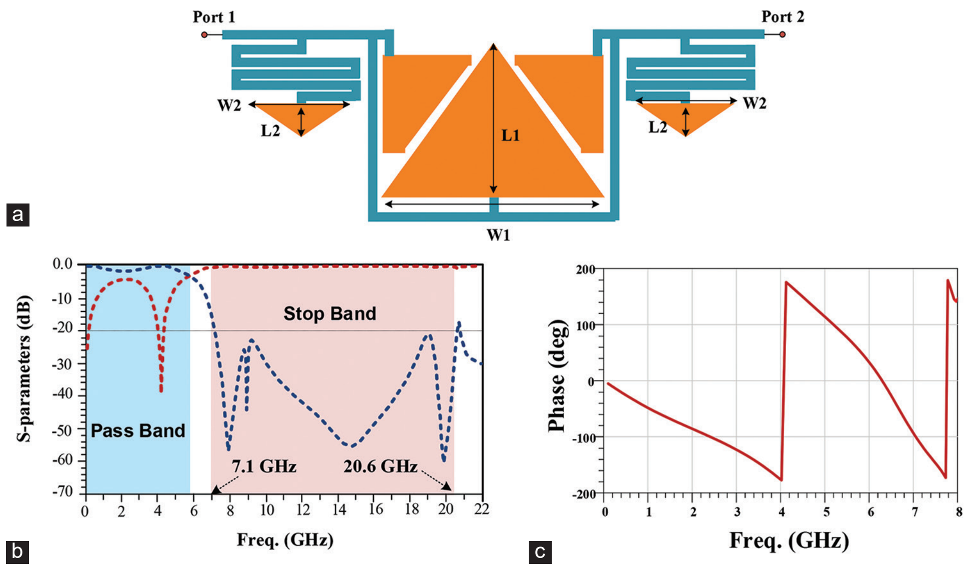

Fig. 3. Structure of the (a) proposed resonator, (b) S-parameters and (c) phase curve of resonator.

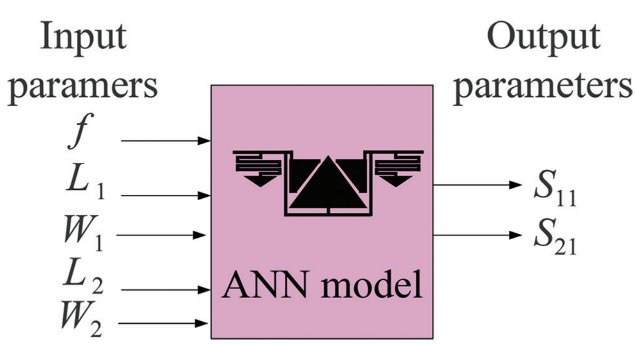

Fig. 4. The provided ANN model for proposed resonator.

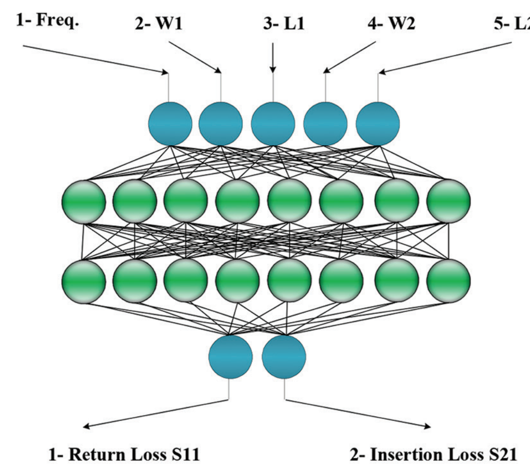

Fig. 5. Structure of the proposed multi-layer perceptron model with 2 hidden layers.

loss) and S_{21} (insertion loss). This configuration allows the ANN to effectively handle the complex dependencies within the design.

The structure of the provided MLP model is illustrated in Fig. 5 as seen the proposed model has 2 hidden layers and each hidden layer has 8 neurons.

To train the model, EM simulation data generated using ADS software were utilized. The training process employed a particle swarm optimization (PSO) algorithm to fine-tune the weights of the network. The data were divided into 80% for training and 20% for testing, ensuring the ANN's ability to generalize to unseen configurations. The performance of the ANN was evaluated using metrics such as mean relative error (MRE) and mean absolute error (MAE), both of which remained below 0.1, indicating a high level of accuracy.

Using the ANN offered several advantages. It significantly reduced the time and computational effort required for iterative simulations, as the trained model could quickly predict the performance of various resonator configurations. This efficiency allowed for rapid exploration of design variations and enabled precise tuning to achieve wideband harmonic suppression with minimal insertion loss.

The MRE, which known, as MRE is determined (Willmott and Matsuura, 2005) in (1) as follow:

TABLE I
PROVIDED MLP MODEL DETAILS

Proposed model details	Specifications
MLP	Type of the artificial neural network
5	Number of neurons in the input layer
2	Number of hidden layers
8	Number of neurons in each hidden layer
2	Number of neurons in the output layer
500	Epochs number
Tansig	Activation functions

MLP: Multi-layer perceptron

$$MRE = \frac{1}{N}\sum_{i=1}^{N}\frac{\left|X_i(Exp) - X_i(Pred)\right|}{X_i(Exp)} \quad (1)$$

The MAE is defined (Armstrong and Collopy, 1993) in (2) as follow:

$$\mathrm{MAE} = \frac{1}{N}\sum_{i=1}^{N}\left|X_i(\mathrm{Exp}) - X_i(\mathrm{Pred})\right|, \quad (2)$$

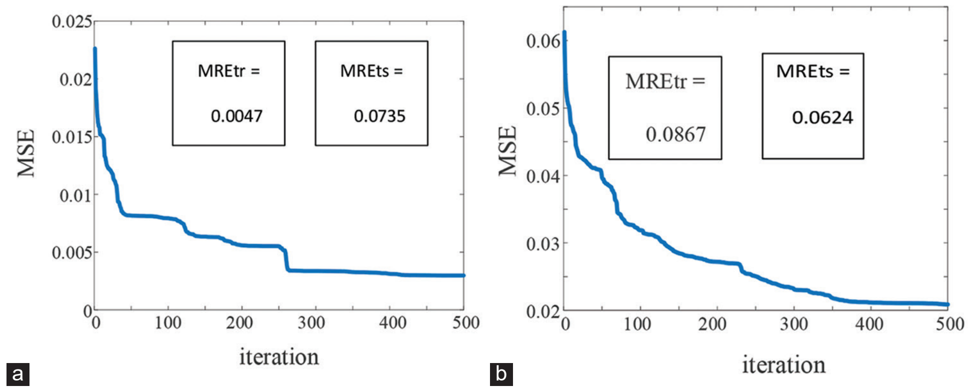

Fig. 6. Obtained value of mean absolute error and mean relative error errors for the (a) S_{11} and (b) S_{21} of the proposed model.

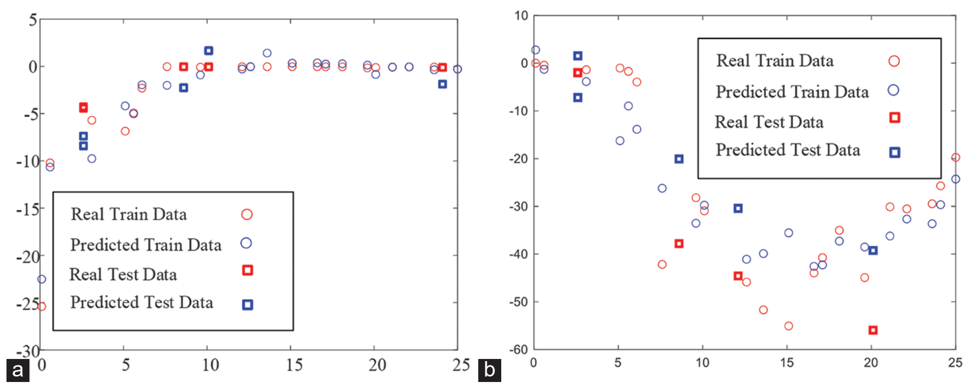

Fig. 7. Real, predicted and test results for the (a) S_{11} and (b) S_{21} of the presented multi-layer perceptron model of the proposed resonator.

The obtained values of MAE and MRE errors of the S_{11} and S_{21} for the provided MLP are listed in the Table II and shown in (Fig. 6a and b), respectively.

The real, predicted, and test results for the S_{11} and S_{21} of the presented MLP model of the proposed resonator are illustrated in (Fig. 7a and b). As results shown the predicted value of the proposed model are very similar to the real values.

The PSO algorithm is selected for the ANN model due to its simplicity, efficiency, and capability to handle complex optimization tasks. PSO operates by mimicking the behavior of natural swarms, where particles explore the solution space by updating their positions based on personal and global best solutions. This approach balances exploration and exploitation, making it well-suited for optimizing the weights and biases of the ANN, which predicts the resonator's S-parameters. Unlike traditional gradient-based methods, PSO effectively navigates non-linear, multi-dimensional spaces, avoiding local minima and achieving global optimization. Its application resulted in a highly accurate ANN model, with a MRE below 0.1, ensuring precise resonator modeling.

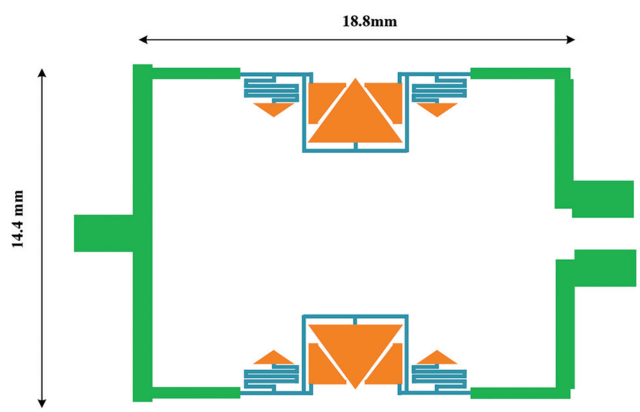

Fig. 8. Structure of the provided dual-band Wilkinson power divider.

TABLE II
Obtained Values of MAE and MRE Errors of the S11 and S21 for the Proposed MLP Model

MRE train error	MRE test error	MAE train error	MAE test error	Output
0.1007	0.0333	0.0735	0.0047	S11
0.2054	0.1103	0.0624	0.0867	S21

MRE: Mean relative error, MAE: Mean absolute error

IV. Proposed WPD

As mentioned in previous sections in the typical divider unwelcome signals at other frequencies are passed with desired signals, which have destructive effects on the main signal. Therefore, to improve the performance of the typical divider, two resonators are applied in the divider structure. The proposed resonator passes signals below 5.8 GHz with very low loss and provide wide rejection band from 7.1 GHz to 20.6 GHz with more than 20 dB suppression level. The structure of the proposed divider is depicted in Fig. 8. The provided DWPD is designed based on RT/Duroid substrate with ε_r = 2.2. The overall size of the proposed divider is

 http://dx.doi.org/10.14500/aro.11945

TABLE III
Performance Summary of the Proposed Dual-Band Divider

Harmonic suppression (suppression level)	Ports isolation loss (dB)	Output return loss (dB)	Input return loss (dB)	Insertion loss (dB)	f_1/f_2 (GHz)
6.8–20.5 GHz (>20 dB)	31/26	34/25	27/21	0.04/0.08	3.6/5.5

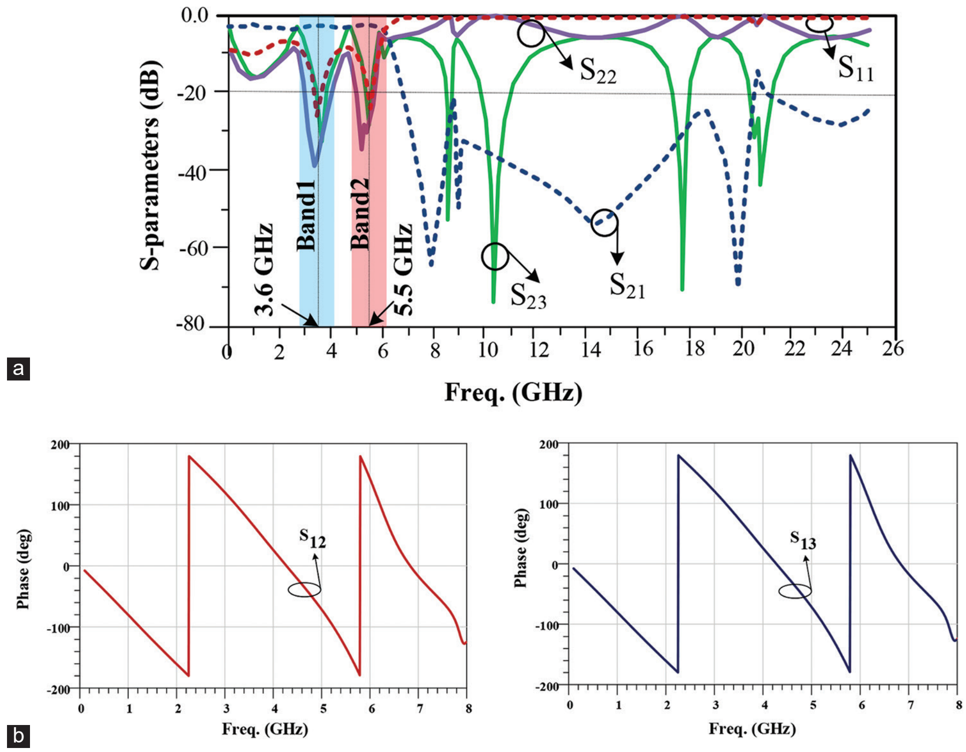

Fig. 9. Frequency response (a) and phase curves (b) of the provided dual-band Wilkinson power divider.

14.4 mm × 18.8 mm, which is equal to $0.23\lambda_g \times 0.31\lambda_g$, where λ_g is electrical wavelength at 3.6 GHz.

The frequency response of the provided DWPD is illustrated in (Fig. 9a). As seen proposed DWPD correctly works at 3.6 GHz and 5.5 GHz. The insertion losses at both operating bands are <0.1 dB. The input and output return losses at both operating bands are better than 20 dB, and better than 25 dB output port isolations are obtained for both operating bands. The results show that provided DWPD has good performance at both operating frequency bands. Also, the proposed dual-band divider has an excellent performance at higher frequencies. The proposed DWPD provides wide harmonics suppression band from 6.8GHz to 20.5GHz with more than 20 dB suppression level, which satisfactory overcome main drawback of the typical divider. The phase curves of the provided DWPD are depicted in (Fig. 9b).

The proposed WPD has the potential to bring exciting advancements to the field of microwave circuit design. It's particularly well-suited for modern applications like wireless communication systems, radar technologies, and signal processing, where maintaining signal quality and filtering out unwanted interference across multiple frequencies is essential.

A performance summary of the provided DWPD is listed in Table III. The results show the good performance of the proposed divider in operating bands and higher frequencies.

V. Conclusion

A DWPD is designed in this paper using triangular-shaped resonators and meandered lines. Applied resonator provides wide suppression band from 7.1 GHz to 20.6 GHz with 20dB attenuation level. The proposed DWPD works at 3.6 GHz and 5.5 GHz with <0.1 dB insertion loss at both operating bands. The input (S_{11}) and output return losses (S22, S33) and ports isolation (S23) parameters at both bands are better than 20dB, which show good performance of the divider at operating bands. The proposed DWPD not only has good performance at two operating bands, but also provides wide suppression band from 6.8 GHz to 20.5 GHz with more than 20dB attenuation level.

Moreover, applied resonator is modeled with neural network. The proposed neural network has two outputs (S_{11} and S_{21}), and two hidden layers with 8 neurons at each layer. The weights of each neuron are obtained using PSO algorithms. The proposed neural network model has accurate results and MRE for the train and test data for both outputs are <0.1, which validates the accurate results of the proposed model.

References

Ahmed, U., and Abbosh, A., 2015. Modified Wilkinson power divider using coupled microstrip lines and shunt open-ended stubs, *Electronics Letters,* 51(11), pp.838-839.

Armstrong, J., and Collopy, F., 1993. Error measures for generalizing about forecasting methods: Empirical comparisons. *International Journal of Forecasting*, 8(1), 69-80.

Bavandpour, S.K., Roshani, S., Pirasteh, A., Roshani, S., and Seyedi, H., 2021. A compact lowpass-dual bandpass diplexer with high output ports isolation. *AEU-International Journal of Electronics and Communications,* 135, pp.153748.

Cheng, K.K.M., and Ip, W.C., 2010. A novel power divider design with enhanced spurious suppression and simple structure. *IEEE Transactions on Microwave Theory and Techniques,* 58(12), pp.3903-3908.

Cheng, K.K.M., and Law, C., 2008. A novel approach to the design and implementation of dual-band power divider. *IEEE Transactions on Microwave Theory and Techniques*, 56(2), pp.487-492.

Heydari, M., and Roshani, S., 2017. Miniaturised unequal Wilkinson power divider using lumped component elements. *Electronics Letters,* 53(16), pp.1117-1119.

Heydari, M., Rostami, P., and Roshani, S., 2019. Design of a modified wilkinson power divider with size reduction and harmonics suppression using triangle-shaped resonators. *Wireless Personal Communications*, 109(3), pp.1571-1579.

Huang, W., Liu, C., Yan, L., and Huang, K., 2010. A miniaturized dual-band power divider with harmonic suppression for GSM applications. *Journal of Electromagnetic Waves and Applications*, 24(1), pp.81-91.

Jamshidi, M., Lalbakhsh, A., Lotfi, S., Siahkamari, H., Mohamadzade, B., and Jalilian, J., 2020. A neuro-based approach to designing a Wilkinson power divider. *International Journal of RF and Microwave Computer-Aided Engineering*, 30(3), pp.e22091.

Jamshidi, M., Siahkamari, H., Roshani, S., and Roshani, S., 2019. A compact gysel power divider design using U-shaped and T-shaped resonators with harmonics suppression. *Electromagnetics*, 39(7), pp.491-504.

Liang, J.G., and Xu, H.X., 2012. Harmonic suppressed bandpass filter using composite right/left handed transmission line. *Journal of Zhejiang University Science C*, 13(7), pp.552-558.

Lin, C.M., Su, H.H., Chiu, J.C., and Wang, Y.H., 2007. Wilkinson power divider using microstrip EBG cells for the suppression of harmonics. *IEEE Microwave and Wireless Components Letters*, 17(10), pp.700-702.

Lotfi, S., Roshani, S., and Roshani, S., 2020. Design of a miniaturized planar microstrip Wilkinson power divider with harmonic cancellation. *Turkish Journal of Electrical Engineering and Computer Sciences*, 28(6), pp.3126-3136.

MahdiAbadi, S., Roshani, S., Parandin, F., and Roshani, S., 2024. Design of a miniaturized 90-degree quadrature hybrid coupler with harmonic suppression ability using π-shaped lumped elements. *Scientific Reports*, 14(1), pp.26489.

Mohammadi, N., Moloudian, G., Roshani, S., Roshani, S., Parandin, F., and Lalbakhsh, A., 2024. A Wilkinson power divider with harmonic suppression through low-pass filter for GSM and LTE applications. *Scientific Reports*, 14(1), pp.2429.

Pirasteh, A., Roshani, S., and Roshani, S., 2020. Design of a miniaturized class F power amplifier using capacitor loaded transmission lines. *Frequenz*, 74(3-4), pp.145-152.

Roshani, S., Dehghani, K., and Roshani, S., 2019a. A lowpass filter design using curved and fountain shaped resonators. *Frequenz*, 73(7-8), pp.267-272.

Roshani, S., Golestanifar, A., Ghaderi, A., Siahkamari, H., and Abbott, D., 2018. High performance microstrip low pass filter for wireless communications. *Wireless Personal Communications,* 99, pp.497-507.

Roshani, S., Hayati, M., Setayeshi, S., Roshani, S., and Mohamadpour, G., 2016. A miniaturized harmonic suppressed power amplifier integrated with lowpass filter for long term evolution application. *Analog Integrated Circuits and Signal Processing*, 89, pp.197-204.

Roshani, S., Jamshidi, M.B., Mohebi, F., and Roshani, S., 2021. Design and modeling of a compact power divider with squared resonators using artificial intelligence. *Wireless Personal Communications,* 117, pp.2085-2096.

Roshani, S., Koziel, S., Roshani, S., Hashemi Mehr, F.S., and Szczepanski, S., 2022. Design and implementation of a dual-band filtering Wilkinson power divider using coupled T-shaped dual-band resonators. *Energies*, 15(3), pp.1189.

Roshani, S., Koziel, S., Yahya, S.I., Chaudhary, M.A., Ghadi, Y.Y., Roshani, S., and Golunski, L., 2023. Mutual coupling reduction in antenna arrays using artificial intelligence approach and inverse neural network surrogates. *Sensors*, 23(16), pp.7089.

Roshani, S., Roshani, S., and Zarinitabar, A., 2019b. A modified Wilkinson power divider with ultra harmonic suppression using open stubs and lowpass filters. *Analog Integrated Circuits and Signal Processing*, 98(2), pp.395-399.

Rostami, P., and Roshani, S., 2018. A miniaturized dual band Wilkinson power divider using capacitor loaded transmission lines. *AEU-International Journal of Electronics and Communications,* 90, pp.63-68.

Srisathit, S., Chongcheawchamnan, M., and Worapishet, A., 2003. Design and realisation of dual-band 3 dB power divider based on two-section transmission-line topology. *Electronics Letters*, 39(9), pp.723-724.

Tang, C.W., and Chen, J.T., 2016. A design of 3-dB wideband microstrip power divider with an ultra-wide isolated frequency band. *IEEE Transactions on Microwave Theory and Techniques,* 64(6), pp.1806-1811.

Wang, X., Ma, Z., Yoshikawa, M., Kohagura, J., Tokuzawa, T., Kuwahara, D., and Mase, A., 2017. Mixed π type structure in W ilkinson power divider design with 3rd harmonic suppression. *Microwave and Optical Technology Letters*, 59(6), pp.1245-1248.

Wang, X., Sakagami, I., Mase, A., and Ichimura, M., 2014a. Trantanella Wilkinson power divider with additional transmission lines for simple layout. *IET Microwaves, Antennas and Propagation,* 8(9), pp.666-672.

Wang, X., Sakagami, I., Mase, A., and Ichimura, M., 2014b. Wilkinson power divider with complex isolation component and its miniaturization. *IEEE Transactions on Microwave Theory and Techniques*, 62(3), pp.422-430.

Willmott, C.J., and Matsuura, K., 2005. Advantages of the mean absolute error (MAE) over the root mean square error (RMSE) in assessing average model performance. *Climate Research*, 30(1), pp.79-82.

Woo, D.J., and Lee, T.K., 2005. Suppression of harmonics in Wilkinson power divider using dual-band rejection by asymmetric DGS. *IEEE Transactions on Microwave Theory and Techniques,* 53(6), pp.2139-2144.

Wu, L., Sun, Z., Yilmaz, H., and Berroth, M., 2006. A dual-frequency Wilkinson power divider. *IEEE Transactions on Microwave Theory and Techniques*, 54(1), pp.278-284.

Wu, L., Yilmaz, H., Bitzer, T., and Berroth, A.P.M., 2005. A dual-frequency Wilkinson power divider: For a frequency and its first harmonic. *IEEE Microwave and Wireless Components Letters,* 15(2), pp.107-109.

Yahya, S.I., Alameri, B.M., Jamshidi, M., Roshani, S., Chaudhary, M.A., Ijemaru G.K., Mezaal, Y.S., and Roshani, S., 2022. A new design method for class-E power amplifiers using artificial intelligence modeling for wireless power transfer applications. *Electronics,* 11(21), pp.3608.

Yahya, S.I., Zubir, F., Hussin, F.A., Chaudhary, M.A., Roshani, S., Sadeghin, J., Jizat, N.M., and Roshani, S., 2024. Design of a compact power splitter with improved performance for wireless applications using recurrent and feed forward neural networks inverted models. *IEEE Access*, 12, pp.117056-117071.